Journal of The Electrochemical Society, **157** (4) H452-H454 (2010)
0013-4651/2010/157(4)/H452/3/$28.00 © The Electrochemical Society

AlGaInP/GaP Heterostructures Bonded with Si Substrate to Serve as Solar Cells and Light Emitting Diodes

Liang-Jyi Yan,[a,c] Chih-Chiao Yang,[a] Ming-Lun Lee,[b,z] Shang-Ju Tu,[a,b] Chih-Sung Chang,[c] and Jinn-Kong Sheu[a,d,z]

[a]*Institute of Electro-Optical Science and Engineering, and* [d]*Advanced Optoelectronic Technology Center and Center for Micro/Nano Science and Technology, National Cheng Kung University, Tainan 70101, Taiwan*
[b]*Department of Electro-Optical Engineering, Southern Taiwan University, Tainan 710, Taiwan*
[c]*High Power Opto Incorporated, Daya Township, Taichung County 42878, Taiwan*

In this study, an AlGaInP/GaP-based heterostructure featuring a silicon substrate and a SiO_2/indium tin oxide/Ag omnidirectional reflector, using a metal-to-metal bonding technique, serves as a dual-function device operating in light emitting and photovoltaic modes. To enhance the light extraction efficiency and conversion efficiency, AlGaInP/Si heterojunction devices with a periodic texture applied to the n–$(Al_{0.5}Ga_{0.5})_{0.5}In_{0.5}P$ surface layer using photolithography and a wet etching process are also presented. Using the light emitting mode and a 350 mA current injection, the external quantum efficiencies of AlGaInP/Si light emitting diodes (LEDs) with (LED-I) and without (LED-II) a textured surface are measured at approximately 17.3 and 11.8%, respectively. The enhancement of the output power in LED-I can be attributed to a multitude of bowl-shaped notches on the surface, resulting in a reduction in the reabsorption probability of photons inside the device because the photon path length of LED-I is shorter than LED-II before photons escape into free space. When devices are operated in a photovoltaic mode, measured under an air mass 1.5 condition, the typical efficiency and fill factor are around 4.67 and 83%, respectively, for devices with a textured surface.
 [DOI: 10.1149/1.3306004]

Manuscript submitted October 14, 2009; revised manuscript received January 4, 2010. Published February 25, 2010.

Surface texturing techniques are available and can be customized to improve light extraction and incident efficiency of semiconductor optoelectronic devices, including light emitting diodes (LEDs) and solar cells.[1,2] In conventional $(Al_xGa_{1-x})_{0.5}In_{0.5}P$ LED emitting wavelengths of 560–670 nm, the light extraction efficiency (LEE) of AlGaInP/GaAs LEDs is low because the downward light is absorbed by the thick GaAs substrate.[1] Although the problem of substrate absorption can be partially resolved by using distributed Bragg reflectors, these only exhibit a narrow band of high reflectivity.[1] AlGaInP LEDs with high levels of brightness, featuring a metal or a Si substrate and a metal reflector layer [an omnidirectional reflector (ODR)], are thus developed to further enhance the LEE of AlGaInP LEDs.[3] The transparent substrate (TS)-type AlGaInP LEDs using wafer-direct bonding technology have been applied for more than a decade. However, such TS-LEDs require a critical and costly GaP wafer-bonding process.[4] For the so-called metal bonding (MB) LEDs,[3] the technical requirements are less strict during the device process vs the wafer-direct bonding process.[5] In addition to the absorption of the GaAs substrate, critical angle loss, due to large differences between the high refractive-index semiconductor material and the lower refractive-index surrounding material, i.e., air or resin, is also a crucial issue. To enhance the escape probability of photons generated in the active layer of the LED, a large critical angle or a rough surface is required.[1,6] Although the refractive index of a semiconductor cannot be changed, one can enhance the LEE by roughening the semiconductor surface. For an LED, the angular randomization of photons can be achieved through surface scattering on the roughened top surface of the LED. Therefore, roughening the surface of an LED is one method for overcoming the total internal reflection of the light inside. In this study, the possibility of whether LEDs with high levels of brightness can serve as potential solar cells or not, including limitations, has been evaluated. The conversion efficiency of a solar cell illuminated at a given spectrum partly depends on the fraction of incident lights. The above-mentioned MB AlGaInP LEDs feature a series of bowl-shaped recesses on the surface formed by wet chemical etching and enhance light absorption when operated in the photovoltaic mode because the reflections inside the recess allow for a second or even a third chance for absorption. For the LED mode, a Ag layer is also placed between the AlGaInP-based epitaxial layers and the Si substrate to serve as an ODR, preventing absorption through an opaque substrate or bonding metal, i.e., indium. Related process steps and results are addressed in the following paragraphs.

[z] E-mail: minglun@mail.stut.edu.tw; jksheu@mail.ncku.edu.tw

Experimental

In this study, AlGaInP LED wafers were epitaxially grown using a metallorganic vapor deposition on a GaAs (100) substrate with a 15° misorientation angle toward the [110] direction. The AlGaInP LED epitaxial structure consisted of an n-type 2 μm thick $(Al_{0.5}Ga_{0.5})_{0.5}In_{0.5}P$ layer, an n-type 0.5 μm thick $Al_{0.5}In_{0.5}P$ layer, a 20-pair $Ga_{0.5}In_{0.5}P/(Al_{0.7}Ga_{0.3})_{0.5}In_{0.5}P$ multiple-quantum-well (MQW) structure, and a 0.8 μm thick p-type $Al_{0.5}In_{0.5}P$ layer. Finally, an 8 μm thick p-type GaAs/GaP double-layer window with a thin GaAs layer placed between GaP and $Al_{0.5}In_{0.5}P$ layers was grown on the p-type $Al_{0.5}In_{0.5}P$ layer. The MB process began with the formation of the ODR on the p-GaP top layer. Before the formation of the ODR, AuBe/Au alloy metals were selectively placed in contact with the p-GaP layer to form ohmic contacts. Next, a SiO_2 layer was also selectively deposited between the AuBe/Au contacts, followed by deposition of an indium tin oxide (ITO) layer. The total thickness of the ITO and SiO_2 was 76 nm. Finally, a Ag layer with a thickness of 350 nm was deposited on the ITO layer to achieve the construction of a SiO_2/ITO/Ag ODR. The bonding substrate was a p-type Si(100) substrate. Before performing the bonding process, the surfaces of the Si substrate had a Ti/Au bilayer metal deposited on them to serve as ohmic contacts, i.e., anode electrodes, when the MB process is complete. At this point, a 2.5 μm thick indium layer was also deposited to serve as the bonding layer. Finally, the AlGaInP LED wafer, combining the aforesaid SiO_2/ITO/Ag ODR and the Si wafer, was attached with an adequate holder at 220°C. A metal layer of Ti/W/Pt/Au was also placed between the In bonding layer and the Ag reflector layer to prevent the diffusion of In into the Ag and ITO layer, which would cause a degradation in the ODR's reflectivity. After the MB process, the GaAs substrate was removed by wet etching using an ammonia solution (NH_4OH). Next, a AuGe metal alloy was deposited on the exposed n–$(Al_{0.5}Ga_{0.5})_{0.5}In_{0.5}P$ layer to form ohmic contacts, i.e., cathode electrodes. Figure 1a and b shows the schematic device structure and the top-view image taken by optical microscopy of the AlGaInP/GaP/Si LED. As previously mentioned, a periodic texture was also applied to the top surface to enhance the LEE of the LEDs. The periodic texture was applied to the n–$(Al_{0.5}Ga_{0.5})_{0.5}In_{0.5}P$ layer by the process of photo-

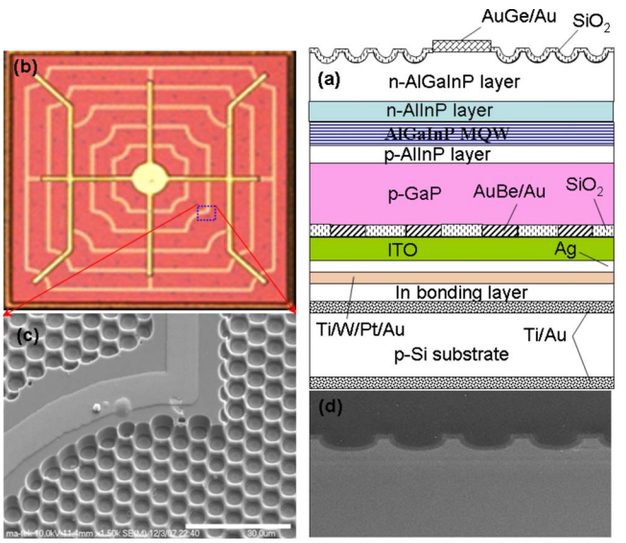

Figure 1. (Color online) (a) The schematic device structure and (b) the top-view image taken by optical microscopy. (c) The enlarged top-view and (d) the cross section view of SEM images of the periodic texture taken from the LED-I.

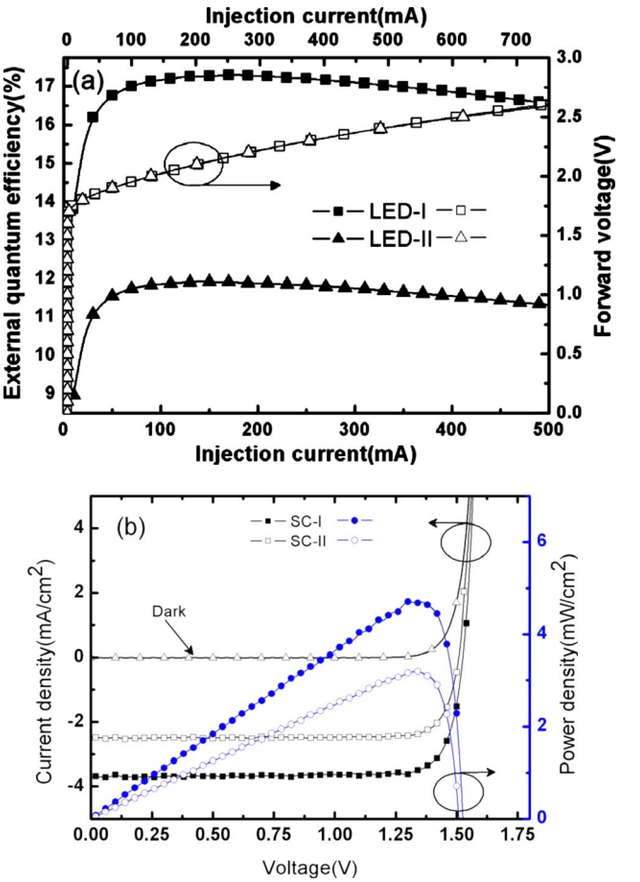

Figure 2. (Color online) (a) The typical characteristics of voltage and external quantum efficiency vs current for LED-I and LED-II with a bare-chip form. (b) The typical characteristics of current density and conversion efficiency vs voltage taken from the SC-I and SC-II under illumination.

lithography and a wet etching using a Br_2 solution. Although the designed dot size and spacing between dots on the photolithography mask was 3 μm, a 5 μm wide bowl-shaped recess was achieved using the isotropic and lateral etching effects. The spacing was reduced to 1 μm, rather than 3 μm. The etching depth of the bowl-shaped recess was approximately 1.5 μm. Finally, an antireflection layer made up of SiO_2 with a thickness of around 0.45 μm was deposited on the top surface. The fractional surface coverage of the AuBe/Au contact and the etched features of the LED were 5 and 62%, respectively. Figure 1c and d shows the enlarged top and cross section views of the SEM images of the periodic texture. In this study, LEDs with a textured surface are labeled LED-I. LEDs with a planar surface were also prepared to be used in comparison and are labeled LED-II. The wafer was cut into individual chips with dimensions of 1000 × 1000 μm. All fabricated LEDs had a dominant emission wavelength of around 635 nm. The current–voltage characteristics of experimental LEDs were measured using the HP-4156C semiconductor parameter analyzer; the output power of LEDs was measured using a calibrated integrating sphere. One sun AM1.5 illumination was provided using a 1000 W Oriel Solar Simulator to evaluate the properties of the AlGaInP/Si heterostructure devices operated in the photovoltaic mode.

Results and Discussion

Figure 2a shows typical characteristics of voltage and external quantum efficiency vs currents for LED-I and LED-II. Forward voltages (V_f) measured at 350 mA are all approximately 2.25 V for both LEDs. This value is comparable with those of conventional LEDs that have not undergone the MB process, i.e., have a GaAs substrate. Although light output power mainly dominates the wall plug efficiency of an LED, electrical properties, such as series resistance, are also key factors consuming part of this input electrical power. The series resistance for LED-I and LED-II are all around 1 Ω. This indicates that the textured process does not lead to degradation in current spreading, which could affect the light output and series resistance. When a 350 mA current injection is used, the typical output power of LED-I and LED-II is measured at around 118 and 81 mW, respectively. This corresponds to an external quantum efficiency of around 17.3 and 11.8% for LED-I and LED-II, respectively, as shown in Fig. 2a. We can enhance the light output power by 45% by applying a periodic texture on the LED-I. The observed enhancement of the output power in LED-I can be attributed to a multitude of bowl-shaped notches on the LED surface, resulting in a reduction in the reabsorption probability of photons because the photon path length is shorter before these photons escape into free space.[1,6]

To evaluate the properties of the above-mentioned devices when they were illuminated at a given condition to measure current density-voltage (J-V) characteristics, a solar simulator is used to render a standard air mass 1.5 condition. Figure 2b shows typical J-V characteristics taken under illumination from LED-I to LED-II. The photocurrent density of devices is far higher than the dark current when the forward bias is lower than 1.5 V. The photovoltaic effect can be clearly observed under illumination, as shown in Fig. 2b. LEDs with and without a textured surface operating in a photovoltaic mode are labeled as SC-I and SC-II, corresponding with LED-I and LED-II, respectively. For SC-II, the typical short-circuit current density (J_{sc}), open-circuit voltage (V_{oc}), and fill factors (FFs) extracted from J-V curves are around 2.5 mA/cm^2, 1.52 V, and 84%, respectively, corresponding to a conversion efficiency of approximately 3.19%. For SC-I, the V_{oc} and FF are almost the same as SC-I. However, J_{sc} of SC-I is approximately 3.7 mA/cm^2, corresponding with a 48% improvement compared to SC-II. This may be attributed to the fact that the enhanced photocurrent is associated with increased light absorption caused by reflections in the surface texture, which allow for a second or even a third chance for absorption. Although its efficiency is far smaller than that of the epitaxial lift-off GaAs solar cells with single junctions,[7] one should remember that the present devices are designed to operate in the light emitting

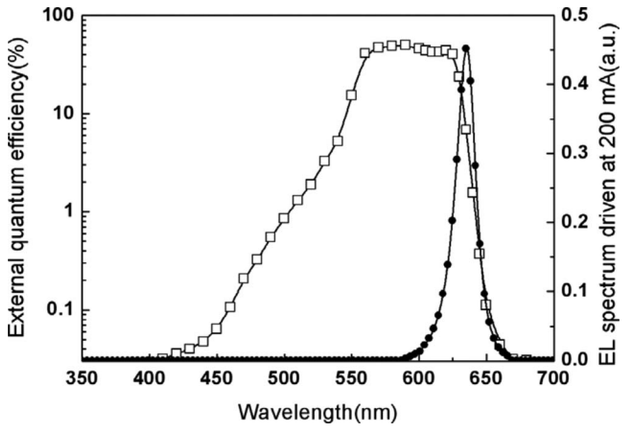

Figure 3. The zero-biased spectral response and the EL spectrum operated at 350 mA taken from SC-I and LED-I, respectively.

and photovoltaic modes. To minimize the absorption of photons emitted from the active layer and the overflow of injected carriers into the cladding layer in LEDs, the active layer is generally clad by materials with a bandgap that is higher than the active layer. This design concept is contrary to that of the solar cell. Considering the layer structures in present devices, the low conversion efficiency observed in SC-I and SC-II may be due to a low absorption efficiency in the underlying layer beneath the active layer (MQW) and the large optical dead space employing severe surface absorption in the topmost layer (n-type AlGaInP layer).[8] The latter case demonstrates an ineffective absorption due to the generated holes recombining with electrons or other charged states before reaching an electrode due to a diffusion length of only a few micrometers for holes in the n-AlGaInP layer. p-AlInP and p-GaP underlying layers with bandgaps higher than the active layer (MQW) have low light absorption because most incident light is blocked by the topmost (n-type AlGaInP layer) and active layers. To clarify this point, the external quantum efficiencies were measured as a function of wavelength. As shown in Fig. 3, one can see that the zero-biased spectral response taken from SC-I shows a distinct bandpass characteristic. The spectral response exhibits a short wavelength and a long wavelength cutoff at around 550 and 635 nm, respectively, which correspond to the surface absorption of the n-AlGaInP layer and the $Ga_{0.5}In_{0.5}P/(Al_{0.7}Ga_{0.3})_{0.5}In_{0.5}P$ MQW layers. As can be seen in the electroluminescence (EL) spectrum, carrier injection into the MQW region leads to an emission peak of around 635 nm, which corresponds to the long wavelength cutoff in the spectral response observed from SC-I, as shown in Fig. 3. The peak value of quantum efficiency is around 50% in the spectral range of 550–635 nm, indicating that the absorption range of the present devices covers only a small portion of the solar spectrum and, hence, a low conversion efficiency. Therefore, one must compromise between the performances of an LED and a solar cell. For example, one can scale down the thickness of the top n-AlGaInP layer to reduce the surface absorption or use a graded bottom p-$Al_xGa_{1-x}As$ layer to replace the p-GaP layer. The latter approach is likely to increase the long wavelength photon absorption.

In summary, an AlGaInP/GaP-based heterostructure featuring a Si substrate and a SiO_2/ITO/Ag ODR using a metal-to-MB technique serves as a dual-function device operating in light emitting and photovoltaic modes. For the LED operation mode, a significant improvement in the light output power of LED-I could be attributed to the periodic texture applied to the $(Al_{0.5}Ga_{0.5})_{0.5}In_{0.5}P$ surface layer, which may effectively increase LEE, compared to LED-II. The periodic texture of a surface may reduce the reabsorption probability of photons because the photon path length in LED-I is shorter than that in LED-II before photons escape into free space. Present devices demonstrate behaviors similar to a solar cell with open-circuit voltage and FF of around 1.52 V and 84%, respectively. Although their efficiency is far smaller than that of an epitaxial lift-off GaAs solar cell, the conversion efficiency would be further boosted if a compromise is made between the performance of an LED and a solar cell.

Acknowledgment

This work has been granted by the Frontier Materials and Micro/Nano Science and Technology Center, NCKU. The authors acknowledge the National Science Council for the financial support and provision of the research grant no. NSC 97-2221-E-006-242-MY3 and no. 98-2221-E-218-005-MY3.

National Cheng-Kung University assisted in meeting the publication costs of this article.

References

1. E. F. Schubert, *Light-Emitting Diodes*, 2nd ed., pp. 150–160, Cambridge University Press, Cambridge, U.K. (2006).
2. S. O. Kasap, *Optoelectronics and Photonics: Principles and Practices*, pp. 269–271, Prentice-Hall, Englewood Cliffs, NJ (2001).
3. Y. J. Lee, H. C. Kuo, S. C. Wang, T. C. Hsu, M. H. Hsieh, M. J. Jou, and B. J. Lee, *IEEE Photonics Technol. Lett.*, **17**, 2289 (2005).
4. F. A. Kish, F. M. Steranka, D. C. Defevere, D. A. Vanderwater, K. G. Park, C. P. Kuo, T. D. Osentowski, M. J. Peanasky, J. G. Yu, R. M. Fletcher, et al., *Appl. Phys. Lett.*, **64**, 2839 (1994).
5. F. A. Kish, D. A. Vanderwater, M. J. Peanasky, M. J. Ludowise, S. G. Hummel, and S. J. Rosner, *Appl. Phys. Lett.*, **67**, 2060 (1995).
6. J. K. Sheu, C. M. Tsai, M. L. Lee, S. C. Shei, and W. C. Lai, *Appl. Phys. Lett.*, **88**, 113505 (2006); see also references therein.
7. J. J. Schermer, P. Mulder, G. J. Bauhuis, P. K. Larsen, G. Oomen, and E. Bongers, *Prog. Photovoltaics*, **13**, 587 (2005).
8. D. J. H. Lambert, M. M. Wong, U. Chowdhury, C. Collins, T. Li, H. K. Kwon, B. S. Shelton, T. G. Zhu, J. C. Campbell, and R. D. Dupuis, *Appl. Phys. Lett.*, **77**, 1900 (2000).